PHYSICAL REVIEW B **109**, 024109 (2024)

Featured in Physics

Experimental investigation of the premelting process in Sn

Stephen G. Lipson[*] and Emil Polturak[†]
Physics Department, Technion-Israel Institute of Technology, Haifa 3200003, Israel

(Received 28 August 2023; revised 12 October 2023; accepted 11 December 2023; published 25 January 2024)

Melting of a real solid involves three stages: first comes surface melting, then the melting of grain boundaries, and finally the melting of the bulk. The first and second stages are often called "premelting." While surface melting and bulk melting have been extensively studied, melting of grain boundaries was not. We developed an optical method which allowed us to study all three stages of melting in pure materials. Using Sn crystals and polycrystals, we were able to detect melting of the grain boundaries inside the solid around 5 K below the bulk melting temperature, and thus lead to a better understanding of how a real solid melts.

DOI: 10.1103/PhysRevB.109.024109

I. INTRODUCTION

The process of melting ice must have been the first phase transition observed by mankind, but it is still not completely understood. One scenario of melting, proposed by Lindemann in 1910 [1], is associated with thermal vibration of atoms about their position inside the solid. According to this scenario, above a certain temperature T_{M} the ratio between the amplitude of these vibrations and the interatomic spacing becomes too large for the solid to remain ordered and melting takes place. This scenario is attractive mostly due to its simplicity, but the actual agreement with experiment is at best qualitative, since this ratio depends on the type of atomic interaction in the solid and its crystal structure, and is found to lie between 0.05 and 0.2 [2]. This has been termed by van der Veen [3] a "homogeneous theory" because it does not take into account nucleation of the liquid phase at preferred sites in the solid. When the solid phase is polycrystalline, it results in a precursor to the melting transition [4]. In general, the appearance of liquid at such preferred sites below the bulk melting transition is called "premelting."

Melting of a pure crystalline solid has been shown both experimentally and theoretically to be a multistage process, which has been reviewed by Dash in 1999 [5]. In a solid of finite size, melting actually starts at the surface. Surface melting was proposed, also in 1910, by G. Tammann (quoted by Dash [5]) and was discovered experimentally by Frenken and van der Veen in 1985 [6,7] who investigated changes of the surface of Pb crystals as a function of temperature and orientation. The onset of surface melting involves a progressive disordering of the atoms in the surface layers since these atoms are less strongly bound than the atoms inside the solid and takes place at a temperature lower than T_{M}. Surface melting has been investigated in several materials using a variety of techniques [6–26].

Another property of a real solid is that, except for very special cases (e.g., graphene), it is invariably composed of an agglomerate of solid grains. Each of these grains may itself be a high-quality crystal, so that neighboring grains are crystals misoriented relative to each other. In what we call macroscopic high-quality single crystals, the degree of misorientation is typically less than 1°. The interfaces between these grains, i.e., grain boundaries, are under additional stress resulting from disorder. As a result, they melt at a temperature lower than T_{M}, a process called "grain-boundary melting" [9,14,27–34]. Following grain-boundary melting, the solid loses its rigidity on a macroscopic scale, but is not yet a fluid. Consequently, melting of a solid is a three-stage process, with surface melting coming first, then grain-boundary melting, and finally melting of the bulk. While surface melting has been extensively investigated, understanding the melting of grain boundaries is still evolving. In this work we investigate experimentally some of the distinct attributes of this process in pure materials.

II. GRAIN-BOUNDARY MELTING

Basically, this process is characteristic of a polycrystalline sample. The various grains in such a sample are crystals with random relative orientations, with an additional energy σ_{gb} per unit area of the interface separating the grains [29]. However, if this surface energy is greater than twice the crystal-liquid surface energy, $\sigma_{\mathrm{gb}} > 2\sigma_{sl}$, it will be preferable energetically to create between the crystals a liquid layer having a thickness which minimizes the total intergrain energy. This thickness depends on the relative orientation of the two grains. The temperature at which this inequality is satisfied for the largest intergrain angle is the grain-boundary-melting temperature. In principle, as pointed out by Torabi Rad *et al.* [29], this is similar to the process of surface melting which occurs when the solid-vapor surface energy is greater than the sum of the solid-liquid and liquid-vapor surface energies, i.e., $\sigma_{sv} > \sigma_{sl} + \sigma_{lv}$. One must remember that the values of the latter two surface energies depend on the thickness of the liquid layer when it is very thin. The experiments described in this paper use the fact that when a grain boundary melts, the liquid so created usually has a larger volume than the solid it replaces. In the case of Sn for example, the densities of the solid and the liquid

---

[*] Corresponding author: sglipson@physics.technion.ac.il

[†] Corresponding author: emilp@physics.technion.ac.il

at $T_{\rm M}$ differ by 4%. As a result, neighboring solid grains within the solid are pushed apart and the whole crystal becomes distorted. As we shall show, this distortion can be detected optically and forms the basis of our detection method.

Grain-boundary melting was studied theoretically and has been simulated using various models [29,31–35]. Experimentally, it has been investigated using transmission electron microscopy in Ni-doped W [31] and in salt-doped ice [9]. On the other hand, experiments on pure aluminum [27] using hot-stage electron microscopy during heating to close to T_m found no signs of grain-boundary melting for temperatures up to $0.999T_m$. In order to provide experimental results which could be related to the simulations, we chose to do experiments on high-purity metals with good thermal conductivity to ensure that the bulk of the sample would be in thermal equilibrium with its surface. After carrying out exploratory experiments on In, Bi, Pb, and Sn, we decided that, so far, the clearest results were obtained with Sn. These results are described below.

III. EXPERIMENTAL TECHNIQUE

Our experimental method is to inspect visually the changes taking place at the surface of the sample as a function of temperature, using the speckle pattern of reflected laser light. The sample is located inside a vacuum chamber on top of a heated support stage. The chamber contained a 95% Ar–5%H_2 mixture at 5 mbar pressure; this is a standard mixture used to prevent surface oxidation in high-temperature applications such as welding.

The system used to make these observations is shown in Fig. 1. Optical access into the chamber was provided by a window mounted at a small angle to the beam axis, so that light reflected by the window itself would not reach the camera. We illuminate the sample surface with a focused 1-mW green laser beam and observe the light scattered from surface irregularities, known as a speckle pattern. When these irregularities change, the speckle pattern changes too. In the temperature range below $T_{\rm M}$, changes in the surface structure are expected to result from surface melting and grain-boundary melting. It is important to point out that the camera was placed so as to observe the light scattered by the sample, avoiding the specularly reflected light. This setting maximizes the visibility of the changes of the speckle pattern.

The topic of speckle patterns is analyzed in detail in the book by Goodman [36], in which an important result is the relationship between the observed contrast of the speckle and the scattering surface, which in turn depend on the relative heights and sizes of randomly situated scattering regions (Chap. 5 and Fig. 5.18 in Goodman's book [36]). In order to determine the sensitivity of the technique for our experiments, we carried out simulations in which a randomly rough substrate was used to scatter the incident laser light of wavelength λ, and the speckle pattern observed in a plane close to the image plane was calculated. Then, a small random change with amplitude d was made to the surface structure, and the speckle pattern recalculated. These two speckle patterns were then spatially correlated. The resulting spatial correlation function shows a strong peak at the origin when the random changes are small. Even when there is no correlation, this function does not fall to zero at points distant from the origin, since what is measured is light intensity, which is a positive definite quantity. Therefore, any two uncorrelated random light distributions will give a positive value to the correlation coefficient. It is the difference between the background and the peak which gives information of the correlation between the two images. The size of the peak is quite insensitive to the substrate surface structure chosen, and is clearly related to the random change between the two images.

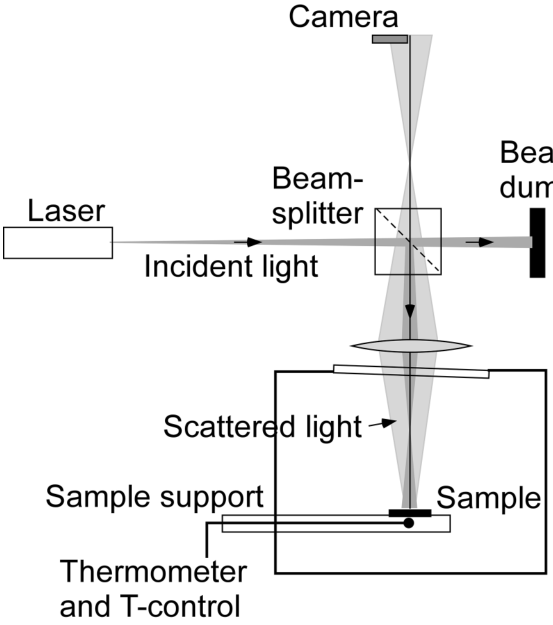

FIG. 1. The experimental system. Light from the laser is partially reflected by the beam splitter, the transmitted part being absorbed by a beam dump. The reflected beam is directed into the vacuum chamber and focused by a lens of focal length 40 mm to a point above the sample surface, so that a region of the sample surface of order about 200 μm diameter is illuminated. The scattered light reflected from the surface is focused by the same lens and detected by a charge coupled device camera.

We calculated the sensitivity of this peak to the amplitude d of the surface changes expected in the experiment. As it turned out, the magnitude of this peak, shown in Fig. 2, was sensitive enough to detect height variations at the surface of order $d = 1$ nm. This is the magnitude of the changes expected from surface melting. Melting of whole grain boundaries should produce much larger changes of the surface and would be easier to detect.

We are interested in detecting changes of the surface with time caused by premelting, namely surface melting or grain-boundary melting. The method we adopted was to acquire two sequential photographs of the speckle pattern of the surface at times separated by typically 120 s and calculate the spatial correlation function $c(x, y)$ between these images. The time difference of 120 s was chosen after watching the camera images of movements of the speckle patterns as a function of temperature and time. It allows us to ignore oscillating fluctuations caused by turbulence in the gas in the chamber, and to concentrate on longer-time changes resulting from changes in the scattering surface itself, which did not oscillate. Several time differences were tried, and 120 s seemed an optimum

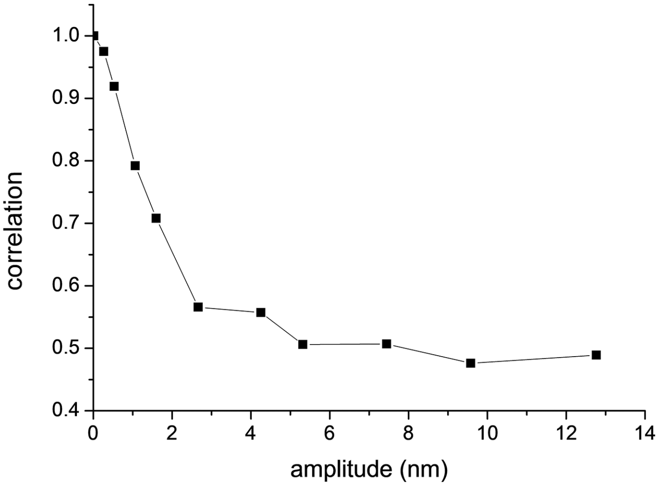

FIG. 2. Maximal correlation between two simulated laser speckle patterns at $\lambda = 532$ nm, scattered by an arbitrary substrate undergoing random height fluctuations of amplitude d.

choice, in which the calculated correlations had a consistent relationship with the visual observations. Examples of such correlation patterns obtained from the surface of a Sn sample can be seen in Fig. 3. Each of these images is acquired at a constant temperature and does not include the specularly reflected laser beam (notice the camera position in Fig. 1). In the analysis, the correlations are normalized so that if the two speckle patterns are identical, the central peak has unit height. Figure 3(a) shows the sample well below the melting point with the surface being static. As the sample is heated, small local changes of the surface broaden the central peak and reduce its height [Fig. 3(b)]. Such changes can result from surface melting. If in addition to the small local changes there is some flow on the surface, the central peak moves from the origin to another position, indicating the flow vector [Fig. 3(c)]. If the flow is not uniform, the central peak splits into several secondary features [Fig. 3(d)].

In the experiments, some light is obviously scattered by other parts of the apparatus (including the beam splitter, the imaging lens, the cell window, and the beam dump). This light makes a constant contribution to the correlation function, in addition to the constant resulting from the positive nature of the light intensity, mentioned earlier. Since we are interested in changes of the surface, we concentrate only on the differences (in time or temperature) between successive images. During the measurements, the temperature difference between the thermometer mounted on the sample stage and the samples themselves was within 1 K.

We tested our method by measuring the correlations of reflected light from the surface of a Pb(110) crystal. Surface melting on Pb(110) was discovered by Frenken and van der Veen [6] in their pioneering work. It started about 100 K below T_M (327 °C). As shown in Fig. 4, we indeed observed a pronounced decrease of the correlations around 230 °C, about

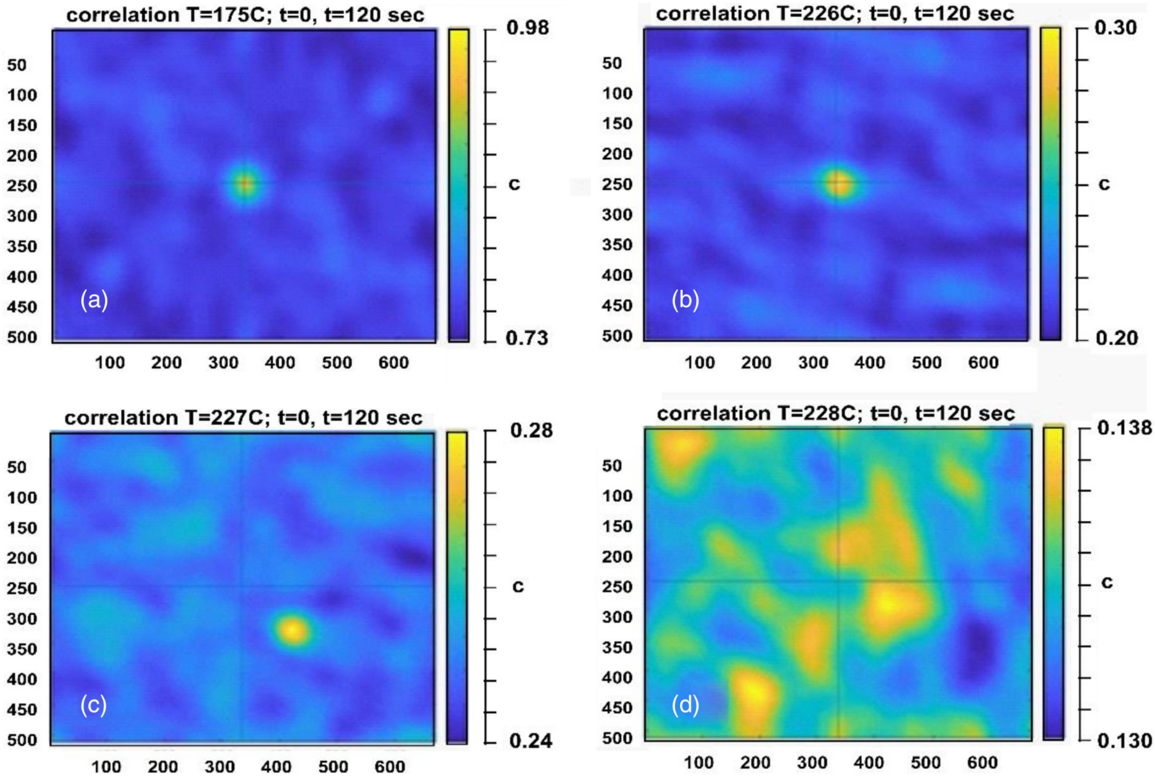

FIG. 3. Examples of two-dimensional spatial correlation between two speckle patterns of light scattered by a Sn sample at several temperatures. The area shown is about 500 μm × 700 μm. It is important to note the differences between the color scales, shown on the right of each picture. Each pair of correlated images was separated by a time interval of 120 s. The temperatures are (a) 175 °C, (b) 226 °C, (c) 227 °C, (d) 228 °C. The bulk melting point is 231.8 °C. While the differences between images (a)–(c) result from surface melting, image (d) at 228 °C is typical of grain-boundary melting.

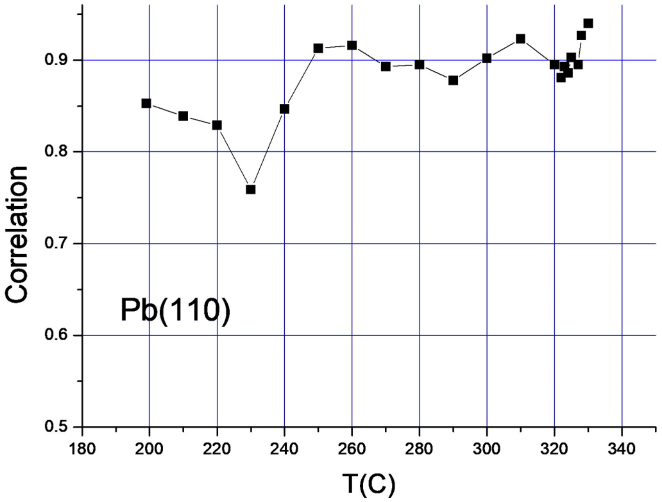

FIG. 4. Temperature dependence of the maximum correlation between speckles of light scattered from a Pb(110) surface. The time interval between the correlated images is 120 s. The dip at 230 °C is interpreted as the onset of surface melting, in agreement with [6] and [7].

100 K below T_M. This observation indicates that the Pb(110) surface starts to change at this temperature, and further confirms that our speckle pattern analysis is suitable for detection of surface melting. Having established the sensitivity of our method, we focused on studying both surface melting and grain-boundary melting of Sn.

A. Scanning electron microscope observations

In addition to the optical measurements, we took scanning electron microscope (SEM) images of the surfaces of some samples before and after melting. As could be expected, these images showed microscopically rough surfaces before melting, becoming very smooth after melting and refreezing. From some of the latter images, we could estimate the size of grains to be about 200 nm. These images were taken at room temperature because of the risk of contamination of the apparatus. It was therefore not possible for us to observe the melting process itself using SEM.

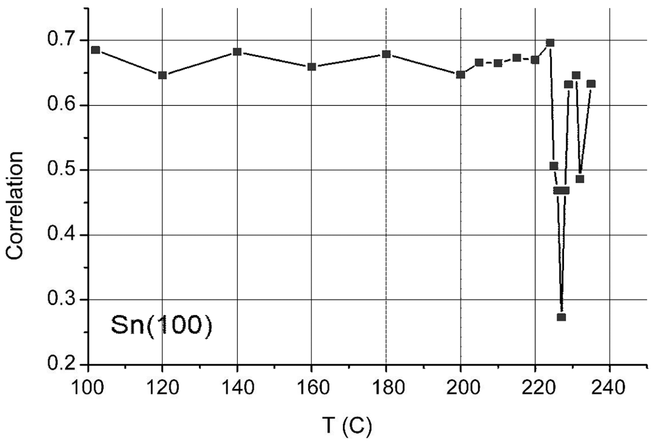

FIG. 5. Maximum value of the correlation between two speckle patterns separated in time by 120 s, as a function of temperature, for a (100) surface of a β-Sn crystal ($T_M = 231.8\,^\circ\mathrm{C}$). We identify the dip between 224 °C and 229 °C as due to grain-boundary melting and that at 232 °C as bulk melting.

B. Experimental results on single Sn crystals and polycrystals

White β-Sn crystals ($T_M = 231.8\,^\circ\mathrm{C}$). were purchased from Princeton Scientific with surface orientations (100) and (110), and had dimensions approximately 1 cm square and 1 mm thickness. In addition, we also measured polycrystalline Sn samples of similar dimensions and varying thicknesses. Polycrystals, made of multitude of misoriented grains, were studied in order to investigate the kinetics of grain-boundary melting. Using both the variations in the magnitude of the correlation peak and the corresponding correlation pictures (Fig. 3) we were able to identify the onset of surface melting, grain-boundary melting, and bulk melting in both single crystals and polycrystals. We were also able to see how the surface orientation of single crystals affected their surface melting. Monitoring the magnitude of the maximum in the correlation plot (as in Fig. 3) is a convenient way of following the surface changes. We show in Fig. 5 the temperature dependence of this correlation on the surface of a (100) Sn crystal.

At temperatures below about 220 °C, the correlation is almost independent of temperature. This implies that outside the noise, in this temperature range the surface is static, the two images which we compare are practically identical, and there is no sign of surface melting. Between 224 °C and 225 °C, the correlations decrease strongly with temperature. Since surface melting affects only the topmost atomic layers, the correlation changes associated with it would be expected to be small (see Fig. 2). The bulk melting temperature is several degrees higher, close to 232 °C. Melting of grain boundaries releases internal stresses inside the solid and causes neighboring grains to shift or rotate relative to one another. In this case, the shape of the whole sample including the surface would be affected. The large correlation change seen around 225 °C is therefore consistent with grain-boundary melting beginning at that temperature. The process begins at the bottom of the sample, which is slightly hotter, being in direct contact with the heating stage. As we increase the temperature very slowly, additional grain boundaries inside the sample melt. This process seems complete at 229 °C, where the correlations become high again. This means that all the grain boundaries are now fluid and there is no stress between neighboring solid grains. In the absence of stress, there is no relative motion of the grains and the surface of the sample appears static. In this situation the correlation over time becomes high again. We identify the correlation minimum at 227 °C as grain-boundary melting. Once we reach the bulk melting temperature close to 232 °C, the whole sample changes and the correlations decrease again. Finally, the degree of correlations after melting (last data point) increases again because the metal is now fluid. In equilibrium, the surface of a fluid is static and so the correlations over time are higher.

We next show the correlation data obtained with a Sn single crystal having a (110) surface orientation (Fig. 6). In this case we see that the correlations start to decrease at much lower temperatures, above 140 °C. We interpret these changes as a result of the onset of surface melting. Between 140 °C

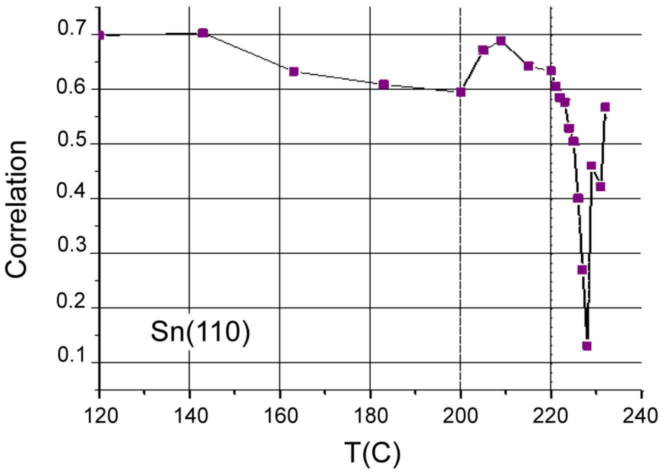

FIG. 6. Maximum value of the spatial correlation between two speckle patterns separated in time by 120 s, as a function of temperature, for laser light reflected from the (110) surface of a β-Sn crystal. We identify the dip between 140 °C and 210 °C as due to surface melting and that between 224 °C and 229 °C as due to grain-boundary melting.

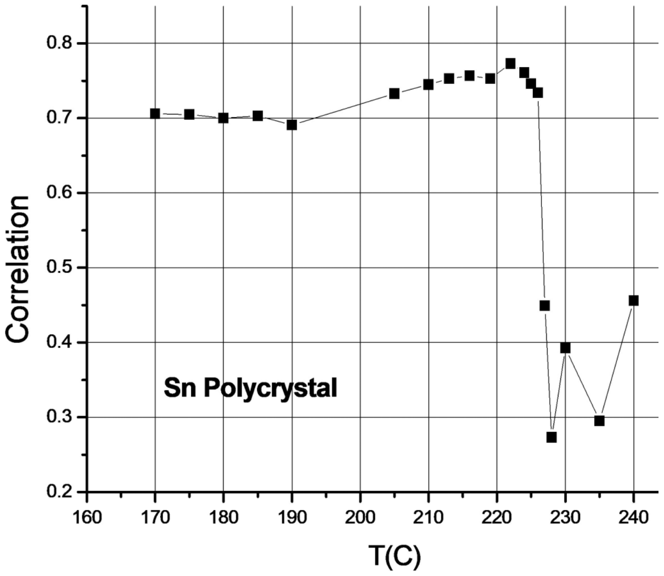

FIG. 7. Maximum value of the spatial correlation between two speckle patterns separated in time by 120 s, as a function of temperature, for laser light reflected from the surface of a β-Sn polycrystal. We identify the dip between 226 °C and 230 °C as due to grain-boundary melting.

and about 200 °C the correlation decreases, meaning that the surface disorders with increasing temperature. Above 200 °C, this trend is reversed and the correlation starts to increase with temperature. We interpret this change as an indication of the completion of a fluid layer on the surface. The surface of a fluid is static, and this is what we believe causes the correlations to increase. At higher temperature around 225 °C the correlations decrease strongly, in the same way as in the case of Sn(100) crystal because of the onset of grain-boundary melting. Finally, as in the case of the (100) crystal, the whole sample melts at T_{M} close to 232 °C.

It is interesting to point out that surface melting on the Sn (110) surface begins almost 100 K below T_{M}, which is similar to what was reported by Frenken and van der Veen [6] for the Pb(110) surface.

When comparing Figs. 5 and 6, one can see that surface melting occurs on Sn at the (110) surface but not at the (100) surface. This observation can be compared with numerical studies of Bavli *et al.* on Mg [37], and of Sorkin *et al.* on V [38], which show that surface melting often begins at the surface having the lowest atomic density.

Since in a polycrystal there should be grain boundaries with higher angles between the grain orientations than in "single" crystals, one might expect grain-boundary melting to initiate at a lower temperature in polycrystals. We investigated several Sn polycrystals. The results, an example of which is shown in Fig. 7, do not support this expectation. In all of the 20 experiments which we carried out on Sn samples, both crystalline (110) and (100) as well as polycrystalline, we found a minimum correlation at 228 ± 1 °C which we attribute to grain-boundary melting.

C. Kinetics of grain-boundary melting in Sn

In our study of single and polycrystals (Figs. 5–7), melting of grain boundaries manifested itself as a large and abrupt change of the degree of correlation. Our understanding of such an event is that once the grain boundaries become fluid, grains can reorient themselves to lower their interface energy. This internal reorientation changes the shape of the crystal, including the profile of its surface. Consequently, the correlation of the speckle pattern from the surface with the one taken before the onset of grain-boundary melting will decrease. The large decrease of correlations seen in Figs. 5–7 above 225 °C is the combined effect of many of the grain boundaries in the sample melting at once. To understand it in more detail, we wanted to detect the melting of individual grain boundaries.

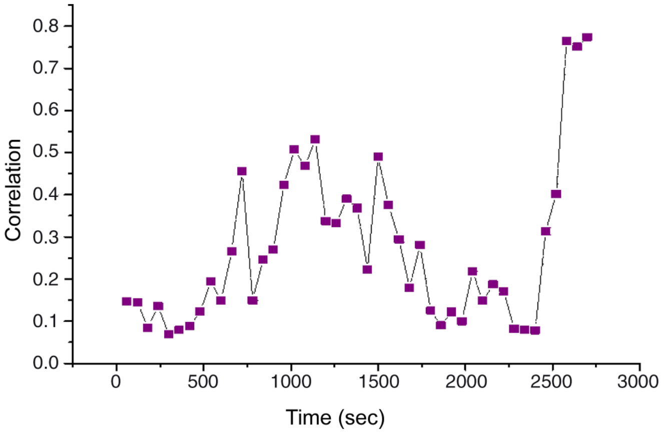

FIG. 8. Time dependence of the correlation of speckle patterns over successive 60-s intervals during grain-boundary melting of a polycrystalline sample, 1.1 mm thick. The temperature at the bottom of the sample was maintained at 230 °C. If a grain boundary melts during the time between frames, the correlation will decrease. If nothing happens during that time, the correlation will increase. This explains the ups and downs of the data shown. Once all the GB's in the sample have melted (after about 2500 s), the sample does not change any more, the correlations increase and remain high.

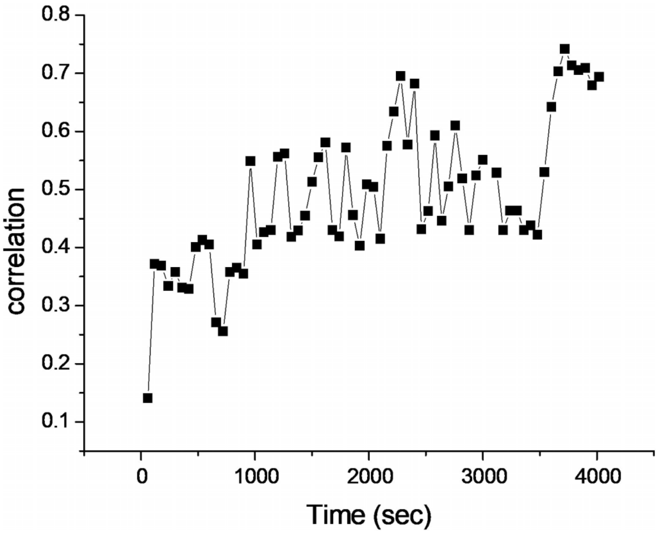

FIG. 9. Time dependence of the correlation of the speckle pattern over successive 60-s intervals during grain-boundary melting inside a 1.4-mm-thick polycrystalline Sn sample maintained at 229 °C. The high correlation after 3500 s indicates that all the grain boundaries in this sample have melted.

To this end, we prepared polycrystalline Sn samples of different thicknesses. These samples are essentially aggregates of grains with a wide range of orientations, and should exhibit properties associated with the dynamics of melting of grain boundaries.

In order to detect melting of individual grain boundaries we used the fact that the bottom of the sample, which is in direct contact with the heating stage, is always slightly hotter than the top. Therefore, once the heating stage reaches the melting temperature of the grain boundaries, grain boundaries at the bottom of the sample will begin to melt. As the temperature rises, this melting front will proceed upwards within the sample towards the free surface. Each time this melting front reaches another grain boundary, some of the frozen-in stress is released and the sample shape should change slightly. To follow these changes, we photographed the speckle pattern every 60 s. This change of the sample shape would lower the correlation with the previous image of the surface. If on the other hand there is no melting of a grain boundary during the time interval from the previous image, the surface would retain its structure and the correlation would increase. These differences offer a convenient way to follow the kinetics of grain-boundary melting.

The maximum correlation between successive images is shown as a function of time. In Fig. 8 we show data for a polycrystal sample 1.1 mm thick, and in Fig. 9 for one 1.4 mm thick. The temperature of the heating stage was 230 °C and 229 °C respectively. The initial low value of the correlation seen in these figures reflects the sharp drop associated with the onset of grain-boundary melting. As proposed above, further changes in the correlation with time depend on whether another grain boundary in the illuminated region has melted during the last 60 s or not. All in all, the correlation would go up and down with time as long as there are grain boundaries in the observed region of the sample which have not yet melted. Once the process is complete, meaning that all the grain boundaries within our sample are fluid, the surface of the sample will become static. The correlations would therefore increase and remain high. We found that the total time for all the grain boundaries in a given sample to melt is proportional to the thickness of the sample.

IV. CONCLUSION

We developed an optical method of observing the processes of surface and grain-boundary melting of reflective metallic samples. We carried out experiments on Sn ($T_{\mathrm{M}} = 231.8\,^{\circ}\mathrm{C}$) which clearly showed the onset of surface-melting on the (110) surface beginning at about 100 K below T_{M}, which is very similar to the results of previous experiments by Frenken and van der Veen [6] on Pb with the same surface orientation. In contrast, Sn crystals with a (100) surface showed no sign of surface melting. We clearly observed melting of grain boundaries taking place at $228 \pm 1\,^{\circ}\mathrm{C}$ in all samples, both single crystal and polycrystal. The observation that the onset temperature of grain-boundary melting is independent of the crystal orientation to within 1 K is surprising and should be investigated using simulations. With the technique we used, it was possible to resolve the melting of individual grain boundaries. We intend to continue this work on other suitable crystals such as Bi. Bi has a much greater crystalline anisotropy. In addition, at its melting temperature solid Bi is less dense than the liquid. These could play interesting roles.

ACKNOWLEDGMENTS

We are grateful to A. Danzig for introducing us into this area of research, to L. Dyumin, A. Eyal, and O. Kleinerman for technical support, and to G. Boussinot for useful discussions. This research was supported by Grant No. 2025208 from the Technion R. & D. Foundation.

---

[1] F. A. Lindemann, Ober die berechnung molekular eigenfrequenzen, Phys. Z. **11**, 609 (1910).

[2] S. Sarkar, C. Jana, and B. Bagchi, Breakdown of universal Lindemann criterion in the melting of Lennard-Jones polydisperse solids, J. Chem. Sci. **129**, 833 (2017).

[3] J. F. van der Veen, Surface-induced melting of solids, in *Phase Transitions in Surface Films* 2, NATO ASI Series Vol. 267, edited by H. Taub, G. Torzo, H. J. Lauter, and S. C. Fain (Springer, Boston, MA, 1991).

[4] J. Kalabinski, A. Drozd-Rzoska, and S. J. Rzoska, Giant premelting effects for solid–liquid discontinuous transition in nitrobenzene under compression, Crystals **13**, 247 (2023).

[5] J. G. Dash, History of the search for continuous melting, Rev. Mod. Phys. **71**, 1737 (1999).

[6] J. W. M. Frenken and J. F. van der Veen, Observation of surface melting, Phys. Rev. Lett. **54**, 134 (1985).

[7] B. Pluis, A. W. Denier van der Gon, J. W. M. Frenken, and J. F. van der Veen, Crystal-face dependence of surface melting, Phys. Rev. Lett. **59**, 2678 (1987).

[8] K. Murata, H. Asakawa, K. Nagashima, Y. Furukawa, and G. Sazaki, Thermodynamic origin of surface melting on ice crystals, Proc. Natl. Acad. Sci. USA **113**, E6741 (2016).

[9] E. S. Thomson, H. Hansen-Goos, J. S. Wettlaufer, and L. A. Wilen, Grain boundary melting in ice, J. Chem. Phys. **138**, 124707 (2013).

[10] M. Elbaum, S. G. Lipson, and J. G. Dash, Optical study of surface melting on ice, J. Cryst. Growth **129**, 491 (1993).

[11] A. Rühm, H. Reichert, W. Donner, H. Dosch, Ch. Grütter, and J. Bilgram, Bulk and surface premelting phenomena in α-gallium, Phys. Rev. B **68**, 224110 (2003).

[12] R. Trittibach, Ch. Grütter, and J. H. Bilgram, Surface melting of gallium single crystals, Phys. Rev. B **50**, 2529 (1994).

[13] A. Danzig, O. Scaly, and E. Polturak, Is the surface fluid during premelting? A study of the surface shear resistance of solid Gallium, Surf. Sci. **705**, 121779 (2021).

[14] A. Alsayed, M. Islam, J. Zhang, P. Collings, and A. Yodh, Premelting at defects within bulk colloidal crystals, Science **309**, 1207 (2005).

[15] Y. Furukawa, M. Yamamoto, and T. Kuroda, Ellipsometric study of the transition layer on the surface of an ice crystal, J. Cryst. Growth **82**, 665 (1987).

[16] X. Wei, P. B. Miranda, and Y. R. Shen, Surface vibrational spectroscopic study of surface melting of ice, Phys. Rev. Lett. **86**, 1554 (2001).

[17] M. Bienfait, J. M. Gay, and H. Blank, Surface premelting of thin films of methane, Surf. Sci. **204**, 331 (1988).

[18] F. Rieutord, R. Simon, R. Conradt, and P. Müller-Buschbaum, Surface melting and preroughening of argon: An X-ray reflection study, Europhys. Lett. **37**, 565 (1997).

[19] D. M. Zhu and J. G. Dash, Surface melting and roughening of adsorbed argon films, Phys. Rev. Lett. **57**, 2959 (1986).

[20] A. W. D. van der Gon, R. J. Smith, J. M. Gay, D. J. O'connor, and J. F. van der Veen, Melting of Al surfaces, Surf. Sci. **227**, 143 (1990).

[21] H. Dosch, T. Höfer, J. Peisl, and R. L. Johnson, Synchrotron x-ray scattering from the Al(110) surface at the onset of surface melting, Europhys. Lett. **15**, 527 (1991).

[22] A. Pavlovska, M. Tikhov, Y. Gu, and E. Bauer, Thermal disordering of the Al(110) surface, Surf. Sci. **278**, 303 (1992).

[23] M. Polčik, L. Wilde, and J. Haase, Partial order of the quasiliquid during surface melting of Al (110), Phys. Rev. Lett. **78**, 491 (1997).

[24] L. Pedemonte, G. Bracco, A. Robin, and W. Heiland, Residual order within the molten Al(110) surface layer, Phys. Rev. B **65**, 245406 (2002).

[25] K. D. Stock, The thickness of molten surface layers on copper monocrystals, Surf. Sci. **91**, 655 (1980).

[26] B. M. Ocko, D. Gibbs, K. G. Huang, D. M. Zehner, and S. G. J. Mochrie, Structure and phases of the Au(001) surface: Absolute x-ray reflectivity, Phys. Rev. B **44**, 6429 (1991).

[27] T. E. Hsieh and R. W. Baluffi, Experimental study of grain boundary melting in aluminum, Acta Metall. **37**, 1637 (1989).

[28] R. Lipowsky, Critical surface phenomena at first-order bulk transitions, Phys. Rev. Lett. **49**, 1575 (1982).

[29] M. Torabi Rad, G. Boussinot, and M. Apel, Dynamics of grain boundary premelting, Nat. Sci. Rep. **10**, 21074 (2020).

[30] Y. Yang, M. Asta, and B. B. Laird, Solid-liquid interfacial premelting, Phys. Rev. Lett. **110**, 096102 (2013).

[31] J. Luo, V. K. Gupta, and D. H. Yoon, Segregation-induced grain boundary premelting in nickel-doped tungsten, Appl. Phys. Lett. **87**, 231902 (2005).

[32] A. Adland, A. Karma, R. Spatschek, D. Buta, and M. Asta, Phase-field-crystal study of grain boundary premelting and shearing in bcc iron, Phys. Rev. B **87**, 024110 (2013).

[33] J. Berry, K. R. Elder, and M. Grant, Melting at dislocations and grain boundaries: A phase field crystal study, Phys. Rev. B **77**, 224114 (2008).

[34] A. Trayanov and E. Tosatti, Lattice theory of surface melting, Phys. Rev. B **38**, 6961 (1988).

[35] W. T. Read and W. Shockley, Dislocation models of crystal grain boundaries, Phys. Rev. **78**, 275 (1950).

[36] J. W. Goodman, *Speckle Phenomena in Optics: Theory and Applications*, 2nd ed. (SPIE, Bellingham, WA, 2020).

[37] P. Bavli, J. Adler, and E. Polturak, Molecular dynamics study of melting of the hcp metal Mg, Phys. Rev. B **84**, 235442 (2011).

[38] V. Sorkin, E. Polturak, and J. Adler, Molecular dynamics study of melting of the bcc metal vanadium. II. Thermodynamic melting, Phys. Rev. B **68**, 174103 (2003).